Attitude Control of Tiltwing Aircraft Using a Wing-Fixed Coordinate System and Incremental Nonlinear Dynamic Inversion

F. Binz*, T. Islam and D. Moormann
RWTH Aachen University, Templergraben 55, 52062 Aachen, Germany

ABSTRACT

In this paper we present a novel concept for robustly controlling the attitude of tiltwing aircraft. Our main contribution is the introduction of a wing-fixed coordinate system for angular acceleration control, which forms the basis of a simple and robust attitude controller. Using the wing-fixed coordinate system allows us to describe the actuator effectivity using simple approximations based on the current operating conditions of the aircraft. Coupled with a robust angular rate control concept, which does not rely on an accurate aerodynamic model, we present a controller stabilizing the entire flight envelope of a tiltwing aircraft. The underlying attitude acceleration controller uses the concept of Incremental Nonlinear Dynamic Inversion (INDI) to achieve robustness against aerodynamic uncertainties. The resulting controller is evaluated in both simulation studies and flight tests.

1 INTRODUCTION

A key goal in the design of many unconventional aircraft types is the combination of efficient forward flight with vertical take-off and landing (VTOL) capabilities. One solution to this problem is the concept of a tiltwing aircraft. These aircraft fly like a conventional airplane in forward flight and achieve VTOL capabilitites by tilting the entire wing upwards to hover.

To stabilize the aircraft in both hover and forward flight several actuators are needed. The aircraft considered here is depticted in Figure 1 and features the following actuators for attitude control: asymmetric thrust of the main motors, ailerons, elevator and thrust of the auxiliary motor. Table 1 shows the primary moments induced by each actuator during hover and forward flight and the corresponding tilt angle. Table 1 hints at a central problem in the design of attitude controllers of tiltwing aircraft: the moments induced by the asymmetric thrust and ailerons change direction between hover and forward flight. Consider the ailerons as an example: During hover flight, at a tilt angle of $90°$, the ailerons primarily induce a yawing moment, since they are positioned in the slip stream of the main engines. However, during forward flight, at a tilt angle of $0°$, the ailerons primarily incude a rolling moment, as in a conventional airplane. In between the hover and forward flight configurations the ailerons incude both a rolling and a yawing moment. Besides the change in direction of the actuator-induced moments, the transition between hover and forward flight is further characterized by potentially highly turbulent airflow behind the main wing. This complicates the design of high-fidelity aerodynamic models, which are needed for many advanced control schemes. Because of these properties, controller design for tiltwing aircraft still presents a challenging problem.

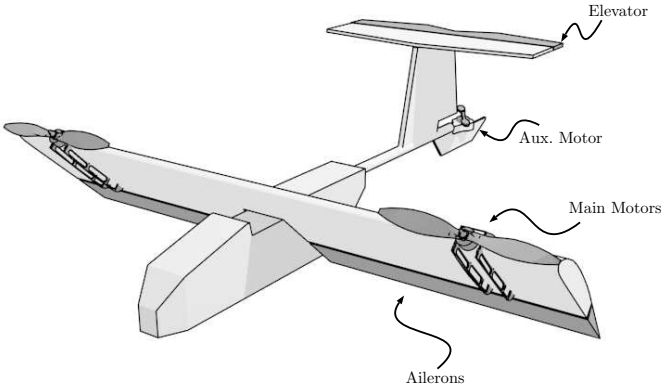

Figure 1: Example tiltwing aircraft in hover configuration

	hover flight	**forward flight**
asym. throttle δ_{asym}	roll	yaw
aux. throttle δ_{aux}	pitch	(-)
ailerons ξ	yaw	roll
elevator η	(-)	pitch
tilt angle σ	$90°$	$0°$

Table 1: Actuator effectivity in hover and tilt configuration

In light of these properties, our main contributions are:

- We observe that the moments induced by the actuators only change direction w.r.t. the body-fixed coordinate system. In the wing-fixed coordinate system the direction of the induced moments is constant. Of course, this simple – and in hindsight obvious – observation by itself does not lead to more robust controllers, but should be

*binz@fsd.rwth-aachen.de

understood as a tool for understanding tiltwing aircraft dynamics and exploring the design space of attitude controllers.

- Inspired by the body of work concerning robust control schemes in recent years (e. g. Incremental Nonlinear Dynamic Inversion (INDI) [6] or Incremental Backstepping [1]), we propose the combination of a wing-fixed coordinate system with an attitude acceleration controller based on the principle of INDI to yield a robust attitude controller. In the spirit of INDI, which is a sensor based control concept, we derive the needed actuator effectivity not on the basis of characteristic maps at certain trimmed flight states, but instead use the available measurements and simple empirical and analytical models to estimate the actuator effectivity in the current operating conditions.

2 The Wing-Fixed Coordinate System

In this paper we are exclusively considering tiltwing aircraft with a single tiltable wing as depicted in Figure 1 and described in [4]. Our approach should however be also applicable to other tiltwing aircraft with only slight modifications (i.e. quad-tiltwing designs [2]).

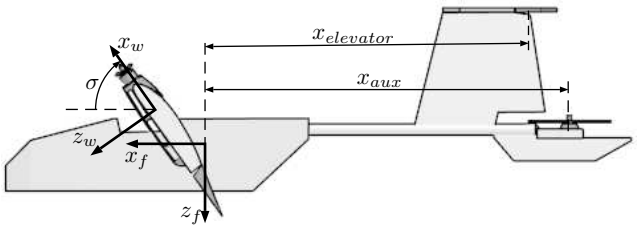

Figure 2: Side view of the aircraft

Figure 2 shows the wing-fixed coordinate system. Conceptually, the origin of the wing-fixed coordinate system lies in the tilt axis of the wing. Since the center of gravity and tilting axis are small, we don't consider the distance between the origins of the body-fixed and wing-fixed coordinate systems in the following treatment.

To transform a vector given in the body-fixed coordinate system (Index b) to the wing-fixed coordinate system, we define the following transformation matrix:

$$T_{wb} = \begin{bmatrix} \cos\sigma & 0 & -\sin\sigma \\ 0 & 1 & 0 \\ \sin\sigma & 0 & \cos\sigma \end{bmatrix} \tag{1}$$

The tilt angle σ assumes a value of ca. $90°$ resp. $0°$ in hover resp. forward flight configuration.

2.1 Transformation of Moment of Inertia

For the scope of this work, we assume that the aircrafts moment of inertia is constant w.r.t. the tilt angle σ. Nevertheless, we need to transform the moment of inertia given in the body-fixed coordinate system into the wing-fixed coordinate system. The moments acting on the aircraft expressed in the body-fixed coordinate system M_b are linked to the body-fixed accelerations $\dot{\Omega}_b$ by the body-fixed moment of inertia J_b:

$$M_b = J_b \cdot \dot{\Omega}_b \tag{2}$$

The body-fixed moments M_b can be expressed in the wing-fixed coordinate system using the transformation matrix T_{wb}:

$$M_w = T_{wb} \cdot M_b \tag{3}$$

$$= T_{wb} \cdot J_b \cdot T_{wb}^{-1} \cdot \dot{\Omega}_w \tag{4}$$

$$\Rightarrow J_w = T_{wb} \cdot J_b \cdot T_{wb}^{-1} \tag{5}$$

Using (5) we calculate the wing-fixed inertia based on the current tilt angle and the body-fixed inertia.

2.2 Actuator Effectivity

We introduced the wing-fixed coordinate system with the main goal of simplifying the description of the actuator effectivity. For attitude control, we are interested in the actuator effectivity concerning the roll, pitch and yaw moments (L, M and N). In this section we will discuss the models we employ for the different actuators available. When modelling the actuator effectivity, we try to find simple models which still result in satisfactory controller performance. We are thus neglecting various effects, the most important of which are:

- No cross-coupling between actuators. Every actuator only induces a moment along one axis in the wing-fixed coordinate system.
- Every actuator is exposed to the same free stream velocity, disregarding effects like downwash from the main wing onto the elevator.

2.2.1 Motor model

We assume that the thrust produced by a fixed-pitch propeller is primarily influced by two factors: the angular velocity of the propeller and the inflow speed. Based on this assumption, we first introduce a thrust model

$$F_{motor} = f(V, \delta) \tag{6}$$

where δ is the throttle signal corresponding to the motor currently considered. Based on prior measurements of electric motors performance, we assume that the angular velocity of a an electric motor is approximately linear to the throttle signal applied to the electronic speed controller. This means, that – lacking a direct measurement of the propeller angular velocity – the throttle signal can be used as an equivalent signal.

The thrust model $F_{motor}(V, \delta)$ can be obtained in different ways. In our work, we obtained the thrust model using a simulation based on semi-analytical formulas supported by empirical static-thrust data. The resulting model is a two-dimensional characteristic map, which we approximate using

a two-dimensional second-order polynomial. The local derivative of this polynomial is then computed online.

We use this motor model for the asymmetric thrust produced by the main motors and the thrust produced by the auxiliary motor. For the auxiliary motor, we make the simplifying assumption, that the inflow is negligible ($V_{aux} = 0$), thus reducing the model complexity further.

The inflow of the main motors is estimated using the currently measured airspeed V_A, transformed into the wing-fixed coordinate system:

$$\vec{V}_{Aw} = \begin{bmatrix} u_{Aw} \\ 0 \\ w_{Aw} \end{bmatrix} = T_{wb} \cdot \begin{bmatrix} V_A \\ 0 \\ 0 \end{bmatrix} \tag{7}$$

Only the x-component u_{Aw} of $\vec{V}_{Aw}$ is used as an input to the thrust model.

Using the lever arms of the main motors, we obtain the following effectivity of the main motors:

$$\frac{\partial N}{\partial \delta_{asym}} = 2 \cdot y_{motor} \cdot \frac{\partial F_{motor}(V, \delta)}{\partial \delta_{asym}}\Big|_{V=u_{Aw}, \delta=\delta_{sym,0}} \tag{8}$$

Here, $\delta_{sym,0}$ denotes symmetric throttle signal in the current controller timestep and y_{motor} denotes the lever arm between the motor and the aircrafts center of mass. The factor 2 accounts for the two motors, one on each side of the aircraft.

Similarly, for the auxiliary motor we obtain:

$$\frac{\partial M}{\partial \delta_{aux}} = x_{aux} \cdot \frac{\partial F_{aux}(V, \delta)}{\partial \delta_{aux}}\Big|_{V=0, \delta=\delta_{aux,0}} \tag{9}$$

2.2.2 Control surfaces

We distinguish between two different kinds of control surfaces: those which are assumed to be completely in the free stream and those which are in the slip stream of a propeller. Both kinds of control surfaces are modeled as thin plates of finite length, where the lift F_{lift} changes with the control surface deflection δ according to the following equation:

$$\frac{\partial F_{lift}}{\partial \delta} = \frac{\rho}{2} V^2 S \cdot 2\pi \cdot \frac{\Lambda}{\Lambda + 2} \tag{10}$$

Here, ρ is the air density, V the inflow speed, S the control surface area and Λ the aspect ratio of the wing corresponding to the control surface.

2.2.3 Elevator

Based on (10) the elevator effectivity with lever arm $x_{elevator}$ is then given by

$$\frac{\partial M}{\partial \eta} = \frac{\rho}{2} V^2 S \cdot 2\pi \cdot \frac{\Lambda}{\Lambda + 2} \cdot x_{elevator} \tag{11}$$

The velocity V is assumed to be equal to the measured aerodynamic speed V_A.

2.2.4 Ailerons

A characteristic feature of the tiltwing configuration we describe here is, that the ailerons are partly within the slip stream of the main motors. To capture this property, the wing is divided into three sections, see Figure 3.

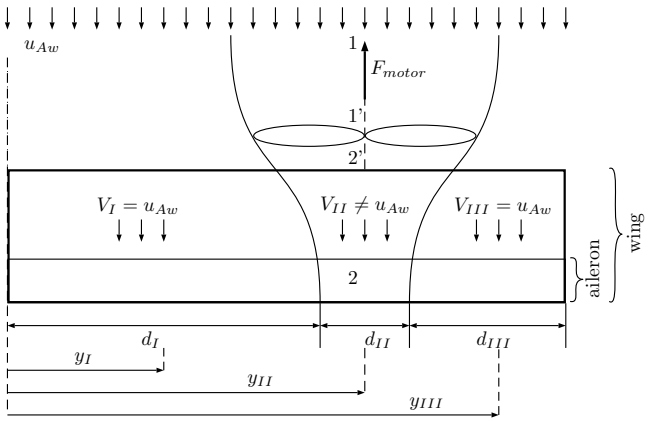

Figure 3: Division of the wing into three sections, with different inflow speeds

Sections I and III are in the free stream and are modeled similar to the elevator, where the free stream speed is used as the inflow speed. Section II is completely in the slip stream of the propeller. Here, the propeller induces an inflow speed even if there is no free stream speed. To estimate this inflow speed, we apply the Bernoulli-Equations along a streamline to the two control volumes $1 \to 1'$ and $2' \to 2$:

$$p_{1'} - p_{2'} = \frac{\rho}{2}(V_1^2 - V_2^2) \tag{12}$$

Multiplying (12) by the propeller area S_{disk} gives the thrust F_{motor} produced by the motor. We assume that the inflow speed equals the free stream speed ($V_1 = u_{Aw}$) and the slip stream is fully developed ($V_2 = V_{II}$).

$$F_{motor} = S_{disk} \frac{\rho}{2}(u_{Aw}^2 - V_{II}^2) \tag{13}$$

This results in the following expression for the inflow speed V_{II} of section II:

$$V_{II} = \sqrt{\frac{F_{motor}(\delta, u_{Aw})}{S_{disk}} \frac{2}{\rho} + u_{Aw}^2} \tag{14}$$

Here, F_{motor} is the thrust obtained by evaluating the thrust model (6) at the current operating point. Using this inflow speed, the effectivity of the ailerons in the slip stream of the motors can be calculated. In total, the effectivity of the ailerons is the sum of the effectivity of the individual sections, resulting in:

$$\frac{\partial M}{\partial \xi} = 2 \cdot \frac{\rho}{2} \cdot 2\pi \frac{\Lambda}{\Lambda + 2} \sum_{i=I..III} V_i^2 \cdot S_i \cdot y_i \tag{15}$$

Again, the factor 2 accounts for the two ailerons.

Summarizing, the moments induced by the actuators are given by:

$$\underbrace{\begin{bmatrix}\partial L\\ \partial M\\ \partial N\end{bmatrix}}_{\partial \vec{M}} = \underbrace{\begin{bmatrix}(15) & 0 & 0 & 0\\ 0 & (11) & (9) & 0\\ 0 & 0 & 0 & (8)\end{bmatrix}}_{M_\delta(u_{Aw},\delta_{sym,0})} \cdot \underbrace{\begin{bmatrix}\partial \xi\\ \partial \eta\\ \partial \delta_{asym}\\ \partial \delta_{aux}\end{bmatrix}}_{\vec{\delta}} \tag{16}$$

3 Attitude Control using Incremental Nonlinear Dynamic Inversion (INDI)

The actuator effectivity described in section 2.2 is needed to apply the concept of INDI to our aircraft. The theory underlying INDI is presented in [6] and [7] and is not repeated here. [6] and [7] are slightly different formulations of INDI, we employ the formulation described in [7]. The central underlying assumption is that the so called *time scale separation principle* holds w.r.t. the actuator dynamics and the dynamics of aerodynamic forces and moments. The control signal can then be computed incrementally using the actuator effectivity matrix M_δ given in (16) using the following formula:

$$\vec{\delta}_{k+1} = \vec{\delta}_k + M_\delta^+ \cdot J_w \cdot (\vec{\nu} - \dot{\vec{\Omega}}) \tag{17}$$

Here, M_δ^+ is the pseudo-inverse of M_δ, which is not invertible due to its dimension and is rank-deficient in hover mode since the elevator effectivity is zero. $\vec{\nu}$ is the pseudo-control input for the INDI control loop and is a vector of commanded angular accelerations. The prospect of INDI as described in [7] is, that closed-loop dynamics from ν_i to $\dot{\Omega}_i$ equals the corresponding actuator dynamics, where i corresponds to the moment axis ($i = x, y, z$). That is, the roll acceleration loop has the dynamics of the aileron actuators. The actuator dynamics are modeled for each actuator individually as first-order lags and are denoted as $A_i(z)$. We note that the pitch axis is actually over-actuated during the transition and fast-forward flight, since both the elevator and the auxiliary motor thrust are effective. For the purposes of designing the attitude controller, we use the slower dynamics of the auxiliary motor to derive attitude controller gains. Figure 4 shows the structure of the

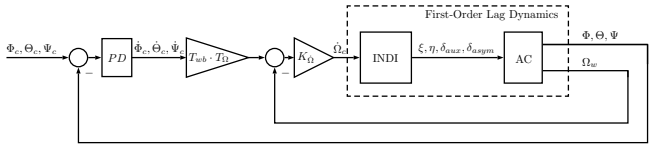

Figure 4: Attitude controller loop

attitude controller. To close the attitude control loop, we use a traditional cascaded approach, where both the angular rates and the attitude angles are fed back using proportional ($K_{\dot{\omega}}$) resp. proportional-derivative (PD) controllers. To generate the wing-fixed commanded angular rates from attitude angle errors, the commanded attitude rates $\dot{\Phi}_c, \dot{\Theta}_c, \dot{\Psi}_c$ are first multiplied by the inverted attitude angle dynamics T_Ω (18) and then transformed into the wing-fixed coordinate system using the transformation matrix T_{wb} (1).

$$\begin{bmatrix}p\\ q\\ r\end{bmatrix} = \begin{bmatrix}1 & 0 & -\sin\Theta\\ 0 & \cos\Phi & \sin\Phi\cos\Theta\\ 0 & -\sin\Phi & \cos\Phi\cos\Theta\end{bmatrix} \cdot \begin{bmatrix}\dot{\Phi}\\ \dot{\Theta}\\ \dot{\Psi}\end{bmatrix} \tag{18}$$

4 Simulation and Experimental Results

To validate the controller design presented in Sections 2 and 3 we first conducted extensive simulation studies. We analyze the perfomance of the attitude controller over the entire flight envelope in Section 4.1. In Section 4.2 we discuss results obtained from flight tests.

4.1 Simulation studies

To conduct the simulation experiments we used the simulation environment described in [5]. The aircraft is modelled as a set of components, where aerodynamic interaction between certain components is simulated to capture the characteristics of tiltwing aircraft.

4.1.1 Stability over entire flight envelope

For tiltwing aircraft, stability during the transition between hover and forward flight is of course of utmost importance. To ensure, that the aircraft is stabilized even when the tilt angle changes quickly, we conducted simulation experiments where the tilt angle is reduced linearly from its hover configuration ($\sigma = 90°$) to its forward flight configuration ($\sigma = 0°$) at different tilt speeds $\dot{\sigma}$. Figure 5 shows the resulting error in the pitch angle over time, normalized to the time when the tilt angle reaches $0°$. Overall, the pitch angle is stabilized very well over the entire flight envelope. The tilt speed $\dot{\sigma}$ intially has a minor effect on the pitch angle error, where faster changes result in higher pitching moments and thus larger pitch angle errors. Still, the maximum pitch angle is below $1°$, which would be a significant improvement compared to previous controller designs for this aircraft.

4.1.2 Attitude controller performance and robustness

Figure 6 shows the step response of the attitude controller in hover configuration, where the computed actuator effectivity is multiplied by different gains to simulate modeling errors. Some cross-coupling between the body-fixed roll and yaw axes exists, mainly because the inverted dynamics (18) does not take the different actuator dynamics into account. In the nominal case ($\times 1.0$) the controller shows satisfactory performance with little oscillations or overshoot. To test the robustness of the attitude controller, we multiplied the calculated actuator effectivity with factors of 0.5 or 1.5 respectively. Despite these large errors in the actuator effectivity, the attitude controller was still stable. Similar to results found in [8],

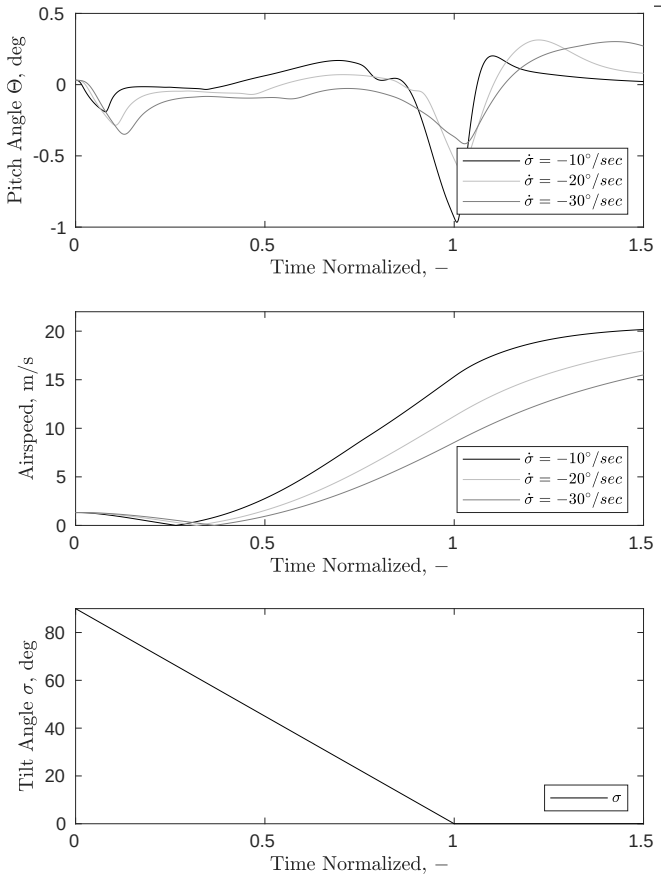

Figure 5: Pitch angle error during transition at different transition speeds (simulation)

assuming a too large actuator effectivity results in a somewhat more sluggish response, while assuming a too small actuator effectivity leeds to fast oscillations.

We conducted similar simulation studies for fast forward flight, see Figure 7. Here, the yaw rate $\dot{\Psi}$ is commanded as $\dot{\Psi}_c = \frac{g}{V_A} \tan \Phi_c$, which is the yaw rate needed for turning without side-slip. Overall, the step responses are still acceptable, but show some overshoot and more sluggish behaviour. We found, that the main cause for this difference is the innermost INDI control loop. Here, the expected accelerations differ significantly from the actual accelerations in fast forward flight. This seems to be a result of quite large damping moments which arise in fast forward flight. In the derivation of INDI these terms are assumed to be negligible. We are currently investigating this issue further to gain deeper understanding and find possible mitigations.

Further robustness analyses, for example against time delays, vibrations, changing actuator dynamics and nonlinearites like saturation in actuator dynamics, were investigated in simulation studies. The results match those already reported in the literature [6, 7, 8] and are thus not repeated here.

Summarizing, we conclude that the presented controller

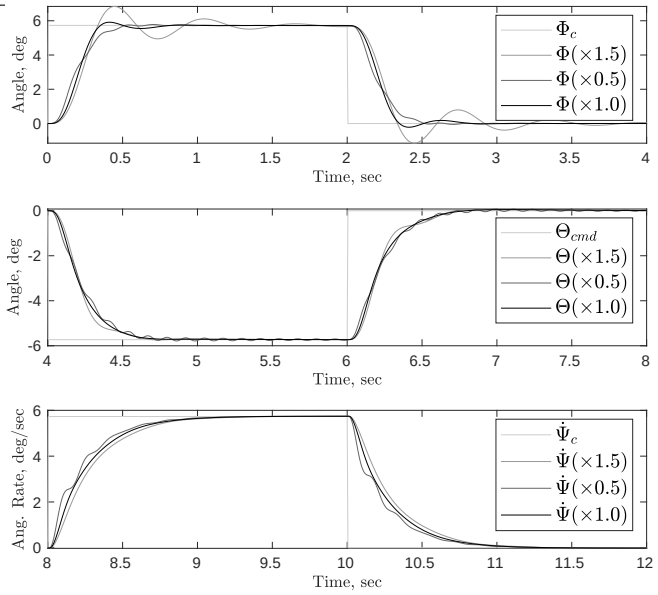

Figure 6: Attitude controller performance in hover flight (simulation)

should be able to robustly stabilize tiltwing aircraft in their entire flight envelope.

4.2 Flight Tests

We conducted the first flight tests in hover flight mode. To assess the performance of the innermost INDI angular acceleration loop, we compared the expected angular accelerations to the measured angular accelerations. The expected angu-

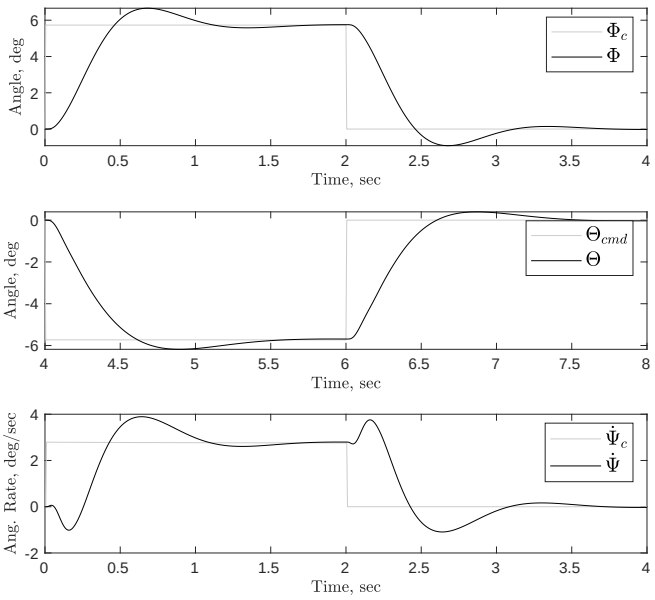

Figure 7: Attitude controller performance in fast forward flight (simulation)

lar accelerations were obtained using the theoretical model of the closed-loop angular acceleration dynamics $A_i(z)$ (see section 3). Figure 8 shows an exemplary timeseries of the wing-fixed yaw and pitch accelerations, $\dot{r}$ resp. $\dot{q}$. It is evident,

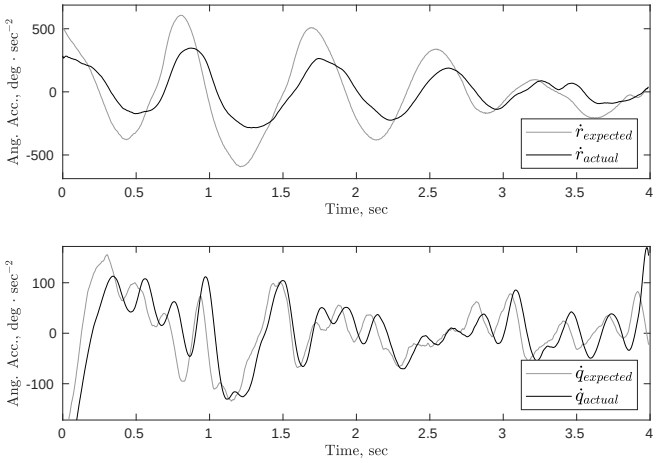

Figure 8: Comparison of expected and actual angular accelerations in hover flight (experiment)

that the wing-fixed yaw accelerations differ significantly from the expected yaw accelerations. We expect that the main cause of this is an inaccurate motor model, which currently does not take the battery voltage into account. Sampling of the characteristic map for the main motor thrust thus results in an overestimation of the effectivity of the asymmetric thrust. Because of this overestimation, the expected acceleration due to asymmetric thrust is higher than the actual acceleration.

The pitch acceleration does not show this particular behaviour, because instead of varying the auxiliary motor speed, the auxiliary motor was operated in a fixed-speed mode with a variable pitch propeller. Thus we expect that the yaw acceleration will improve significantly once the battery voltage taken into account in the thrust model.

The wing-fixed roll accelerations are not shown here, because the effectivity of the ailerons is very low in hover flight. The roll accelerations are thus dominated by the highly turbulent airflow and wind gusts.

Figure 9 shows the performance of the attitude controller described in section 3. Both, the body-fixed roll and pitch axes are stabilized by the controller. Despite the difference in expected and actual wing-fixed yaw acceleration, the performance of the roll controller is satisfactory.

After successful flight tests in hover mode, we conducted further flight tests to validate the controller in the entire flight envelope. Similar to the simulation study summarized in Figure 5, we conducted a transition from hover flight to fast forward flight. Figure 10 shows the roll and pitch angle controller performance during the entire transition phase. The roll and pitch angles were directly commanded by the pilot. The absolute error in roll and pitch angle stays below $3°$ resp. $1°$

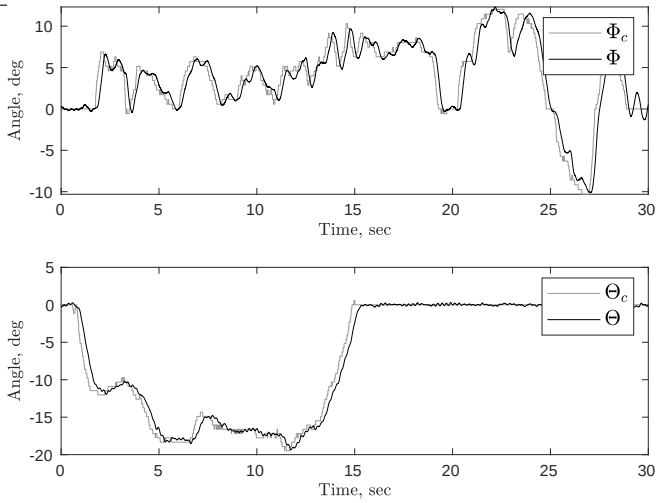

Figure 9: Attitude controller performance in hover flight (experiment)

during the entire transition phase, thus showing a very good correspondence to the simulation studies presented earlier. There are minor oscillations in both pitch and yaw, which are incudced by the controller. Since the controller used to generate these results was not tuned in free flight tests prior these experiments, we are confident that a less agressive parameter selection in the attitude controller will mitigate the oscillations.

We (unintentionally) observed the good robustness properties of the INDI controller during the transition from fast forward flight to hover flight. Figure 11 shows the pilots attempt to transition back into hover flight by increasing the commanded tilt angle from $0°$ to about $45°$ during the first 25 seconds. However, because of the high airspeed of about $19\,\mathrm{m\,s^{-1}}$, the servo responsible for tilting the wing was not able to rotate the wing against the aerodynamic forces. Since there is currently no servo position feedback, the INDI controller assumes that the commanded tilt angle σ_c equals the actual tilt angle (estimated to σ_{est}). Despite the large difference between commanded and actual tilt angle, the INDI still was able to stabilize the aircraft without any noticable perfomance degradation. When further increasing the commanded tilt angle σ_c to about $60°$ from seconds 25 to 30 , the difference between the expected and actual tilt angle evidently became too large, leading to instability.

Starting at second 35 , the pilot began to reduce the airspeed by first reducing the commanded symmetric throttle. At an airspeed of about $17\,\mathrm{m\,s^{-1}}$, the tilt servo was able to overcome the aerodynamic forces, resulting in the wing abruptly tilting up. This abrupt motion of the entire wing of course induces large disturbances, leading to errors of $40°$ and $10°$ in the roll resp. pitch axes. The controller was however able to stabilize the aircraft quickly in about $1\,\mathrm{s}$. In terms of controller performance, we think this incident examplifies the

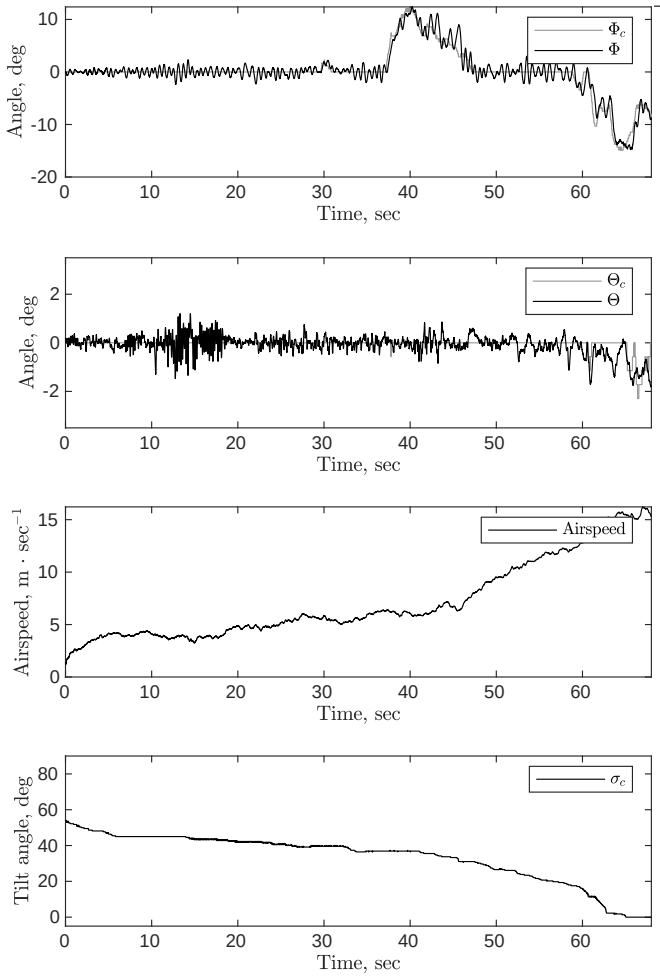

Figure 10: Attitude controller during transition from hover to forward flight (experiment)

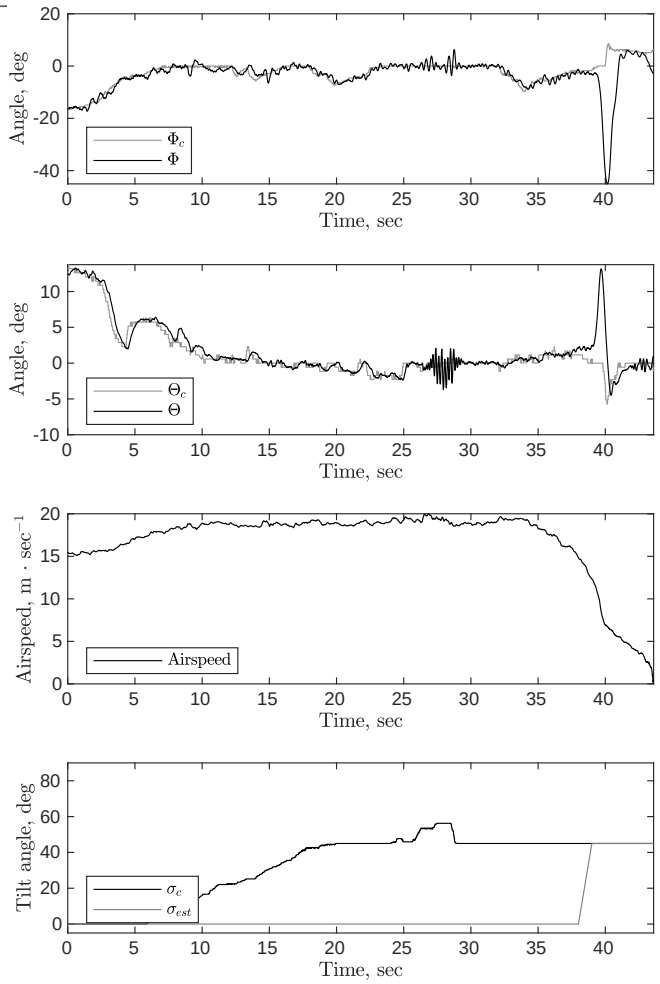

Figure 11: Attitude controller during transition from forward flight to hover (experiment)

good disturbance rejection qualities of the INDI controller.

5 Related Work

The literature offers several alternative approaches for the attitude control of hybrid VTOL aircraft. Naturally, the main differences between the different approaches concern the way in which the highly variable dynamics between hover and forward flight are handled.

In [4] and [2] the aircraft dynamics are linearized around certain trimmed flight states at different airspeeds. This is either done using aerodynamic models of the aircraft or using wind-tunnel measurements. Based on the linearized aircraft dynamics in a flight state a suitable controller can be found. The main assumption made by the authors is that the airspeed is quasi-stationary w.r.t. to the attutide dynamics. Thus, the airspeed can be used as a gain-scheduling variable for the attitude controller. This approach was demomstrated to work well, as long as the underlying assumption of a slowly varying airspeed is met. However, a signficant performance degradation was observed in the aircraft described in [4] once the airspeed varied non-stationary. Also, both approaches are heavily dependent on an accurate aerodynamic model. When obtaining accurate aerodynamic models using wind-tunnel experiments, this results in quite a substantial effort needed once the aircraft is changed (e.g. new wing or fuselage design).

A similar approach to the one we present in this work is found in [3]. Here the authors employ a form of INDI for the attitude control of a tiltrotor aircraft based on the currently measured fight state. However, instead of only considering the actuator effectivity, the incremental change in actuator input $d\delta$ is based on an full aerodynamic model of the aircraft. The authors thus arguably loose some of the benefits of INDI as described in [6, 7] (i. e. robustness against aerodynamic model uncertainty) in favor of a potentially better controller performance. On top of the attitude control itself, the authors also include an actuator allocation procedure to deal with saturations and varying actuator effectivity. Using simulation studies, this approach was reported to show good results over

the entire flight envelope.

6 Conclusion and Future Work

In his work, we presented the application of INDI to a tiltwing aircraft. Using a wing-fixed coordinate system, we derived simple formulas to describe the actuator effectivity with the objective to minimize the dependency on wind-tunnel measurements or high-fidelity aerodynamic models. The resulting formulas only depend on geometric properties of the aircraft and characteristic maps of the thrust produced by the motors, which can be quite easily measured. Thus, this new attitude controller concept should be easily adaptable to changing aircraft designs. The resulting attitude controller showed good performance and robustness properties in simulation studies.

We conducted free flight tests in hover flight mode and obtained similar behaviour to the simulation results. Subsequent flight tests then covered the entire flight envelope from hover flight to fast forward flight. The controller showed good performance in conjunction with good robustness and disturbance rejection qualities.

Future work will concentrate on practical issues like disabling the auxiliary motor during fast forward flight or dealing with actuator saturations in a principled manner.

References

[1] Paul Acquatella B., Erik-Jan Van Kampen, and Q P Chu. Incremental Backstepping for Robust Nonlinear Flight Control. In *Proceedings of the EuroGNC 2013, 2nd CEAS Specialist Conference*, 2013.

[2] Y Beyer, T Krüger, A Krüger, M Steen, and P Hecker. Simulation and Control of a Tandem Tiltwing RPAS Without Experimental Data. In *International Micro Air Vehicle Conference and Flight Competition (IMAV)*, pages 162–169, 2017.

[3] Gabriele Di Francesco and Massimiliano Mattei. Modeling and Incremental Nonlinear Dynamic Inversion Control of a Novel Unmanned Tiltrotor. *Journal of Aircraft*, 53(1):73–86, 2016.

[4] Philipp Hartmann, Carsten Meyer, and Dieter Moormann. Unified Velocity Control and Flight State Transition of Unmanned Tilt-Wing Aircraft. *Journal of Guidance, Control, and Dynamics*, 40(6):1348–1359, 2017.

[5] Marten Schütt, Tobias Islam, Philipp Hartmann, and Dieter Moormann. Scalable Design Approach to Analyse Flight Mechanical Performance for Tiltwing UAVs. In *International Council of Aeronautical Sciences, ICAS, 2018-09-09 - 2018-09-14, Belo Horizonte, Brazil*, 2018.

[6] S Sieberling, Q P Chu, and J A Mulder. Robust Flight Control Using Incremental Nonlinear Dynamic Inversion and Angular Acceleration Prediction. *Journal of Guidance, Control, and Dynamics*, 33(6):1732–1742, 2010.

[7] Ewoud J J Smeur, Qiping Chu, and Guido C H E de Croon. Adaptive Incremental Nonlinear Dynamic Inversion for Attitude Control of Micro Air Vehicles. *Journal of Guidance, Control, and Dynamics*, 39(3):450–461, 2016.

[8] R C van't Veld, E van Kampen, and Q P Chu. Stability and Robustness Analysis and Improvements for Incremental Nonlinear Dynamic Inversion Control. (January), 2018.